

Exact and Monte Carlo study of adsorption of a self-interacting polymer chain for a family of three-dimensional fractals

S Elezović-Hadžić†, I Živić ‡and S Milošević†

†Faculty of Physics, University of Belgrade, P.O.Box 368, 11001 Belgrade, Serbia, Yugoslavia

‡Faculty of Natural Sciences and Mathematics, University of Kragujevac, 34000 Kragujevac, Serbia, Yugoslavia

E-mail: sunchica@net.yu, ivanz@knez.uis.kg.ac.yu, emilosev@etf.bg.ac.yu

Abstract. We study the problem of adsorption of self-interacting linear polymers situated in fractal containers that belong to the three-dimensional (3d) Sierpinski gasket (SG) family of fractals. Each member of the 3d SG fractal family has a fractal impenetrable 2d adsorbing surface (which is, in fact, 2d SG fractal) and can be labelled by an integer b ($2 \leq b \leq \infty$). By applying the exact and Monte Carlo renormalization group (MCRG) method, we calculate the critical exponents ν (associated with the mean squared end-to-end distance of polymers) and ϕ (associated with the number of adsorbed monomers), for a sequence of fractals with $2 \leq b \leq 4$ (exactly) and $2 \leq b \leq 40$ (Monte Carlo). We find that both ν and ϕ monotonically decrease with increasing b (that is, with increasing of the container fractal dimension d_f), and the interesting fact that both functions, $\nu(b)$ and $\phi(b)$, cross the estimated Euclidean values. Besides, we establish the phase diagrams, for fractals with $b = 3$ and $b = 4$, which reveal existence of six different phases that merge together at a multi-critical point, whose nature depends on the value of the monomer energy in the layer adjacent to the adsorbing surface.

PACS numbers: 64.60.-i, 36.20.-r, 05.50.+q

Submitted to: *J. Phys. A: Math. Gen.*

1. Introduction

Statistics of a polymer chain in various types of solvents near an impenetrable wall (boundary) with short-range attractive forces has been extensively studied because of its practical importance [1], and as a challenging problem within the modern theory of critical phenomena [2]. The most frequently applied model for a polymer chain has been the self-avoiding (SAW) random walk model (that is, the walk without self-intersections), so that steps of the walk have been identified with monomers that comprise the polymer, while the solvent surrounding has been represented by a lattice. These problems have been mostly studied for models situated on two-dimensional (2d) Euclidean lattices using various theoretical methods, such as the series expansion method, the renormalization group (RG) techniques, the mean-field approach, Monte Carlo simulations, and the conformal invariance method. In the last two decades these problems have been also studied in a case of fractal lattices embedded in the two-dimensional Euclidean space. On the other hand, in a more realistic three-dimensional case (for the Euclidean lattices, as well as for fractal lattices), a smaller number of results have been obtained. The study of fractal lattices has an advantage not only because their intrinsic self-similarity makes the problem more amenable to an exact approach, but also because these lattices as such may serve to model porous media.

In this paper we report results of our study of a linear polymer situated in the three-dimensional (3d) fractal lattices that belong to the Sierpinski gasket (SG) family of fractals, assuming the interaction between two adjacent nonconsecutive monomers and, in addition, assuming adsorbing interaction with the walls of the fractal interior. This problem has been studied in the case of the 3d Euclidean lattices (see, for instance [3], and references quoted therein), but the number of obtained results is definitely smaller than in the corresponding 2d case. In the 3d case, the main endeavor has been manifested in attempts to establish phase diagrams [3, 4] in the interaction parameter space (which consists of the monomer-monomer interaction parameter and the adsorption energy parameter). In addition to the phase diagram, attempts have been made to calculate critical exponents that characterize various polymer configurations. The first work of this kind for a fractal was done by Bouchaud and Vannimenus [5], who applied the renormalization group (RG) technique for the 3d SG with scale parameter $b = 2$. Here we report results of our exact RG calculation for the 3d SG with $b = 3$ and $b = 4$, and our results for the sequence $2 \leq b \leq 40$ obtained via the Monte Carlo renormalization group (MCRG) method. Therefore, this paper appears to reflect an effort to extend our previous studies performed in the case of the two-dimensional fractal lattices. Such an effort has been incited by the well-known fact that critical properties of a given model depend on dimension of the space in which the model is situated.

This paper is organized as follows. In Sec. 2 we first describe the 3d SG fractals for general b . Then, we present the framework of the RG method for studying the polymer adsorption problem on these fractals (taking into account the presence of the monomer-monomer interaction), in a way that should make the method transparent for

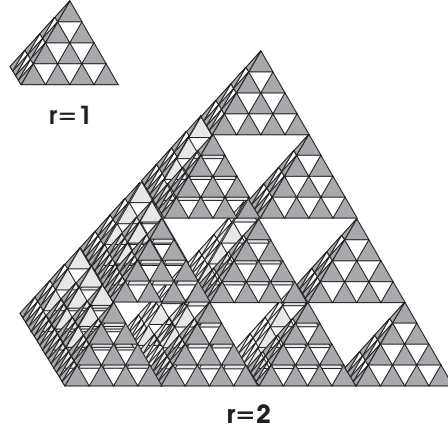


Figure 1. The first two steps ($r = 1$ and $r = 2$) of the self-similar construction of the 3d SG fractals, in the case $b = 4$.

exact calculations, as well as for the Monte Carlo calculations. In Sec. 3 we elaborate on the phase diagrams obtained through the exact RG analysis for the $b = 3$ and $b = 4$ SG fractals, and, in addition, we display our findings for the concomitant critical exponents ν (associated with the mean squared end-to-end distances of polymers) and ϕ (associated with the number of adsorbed monomers). For $b = 3$, values of ν , for different phases, have been previously calculated [6], so that here we report the values for the corresponding crossover exponent ϕ , whereas in the $b = 4$ case we had to calculate values for the both exponents ν and ϕ . In Sec. 4 we explain details of the MCRG calculations of the critical exponents, for arbitrary b , and present their specific values up to $b = 40$. Summary of the obtained results and the relevant conclusions are given in Sec. 5.

2. Renormalization group scheme

Each member of the 3d SG family of fractals is labeled by the scale parameter $b = 2, 3, 4, \dots$ and can be constructed recursively starting with the pertinent generator $G^{(1)}(b)$ which is a tetrahedron of base b , that contains $b(b+1)(b+2)/6$ unit tetrahedrons (see Fig. 1). The subsequent fractal stages are constructed self-similarly, by replacing each unit tetrahedron of the initial generator by a new generator. Thus, to obtain the r th-stage fractal lattice $G^{(r)}(b)$, which we shall call the r th order generator, the recursive process has to be repeated $(r - 1)$ times, so that the complete fractal is obtained in the limit $r \rightarrow \infty$. Fractal dimension d_f of 3d SG fractal is equal to

$$d_f^{3d} = \ln[(b+2)(b+1)b/6] / \ln b. \quad (2.1)$$

We assume here that one of the four boundaries of the SG fractal is impenetrable attractive surface (wall), which is itself a 2d SG fractal with the fractal dimension

$$d_f^{2d} = \ln[b(b+1)/2] / \ln b. \quad (2.2)$$

In order to describe both the effect of monomer-monomer interaction and the effect of attractive (adsorbing) surface, one should introduce the three Boltzmann factors:

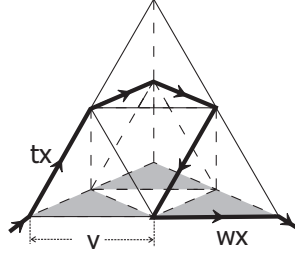


Figure 2. The fractal structure of the $b = 2$ 3d SG fractal at the first stage of construction, with an example of the SAW path. The shaded area at the basis of the tetrahedron represents the adsorption wall. The steps on the adsorbing wall and in the adjacent layer are weighted by the factors $w = e^{-\epsilon_w/T}$ and $t = e^{-\epsilon_t/T}$, respectively. Here ϵ_w is the energy of a monomer lying on the adsorbing wall ($\epsilon_w < 0$), and $\epsilon_t > 0$ is the energy of a monomer that appears in the layer adjacent to the wall. The Boltzmann factor $v = e^{-\epsilon_v/T}$ corresponds to the energy of interaction $\epsilon_v < 0$ between two nonconsecutive neighboring monomers. The depicted SAW path represent one term in equation (2.5) for $r = 1$ with $N = 5$, $P = 4$, $M = 1$ and $K = 2$.

$v = e^{-\epsilon_v/k_B T}$, $w = e^{-\epsilon_w/k_B T}$, and $t = e^{-\epsilon_t/k_B T}$, where ϵ_v is the energy corresponding to interaction between two nonconsecutive neighboring monomers, ϵ_w is the energy of a monomer lying on the adsorbing surface, and ϵ_t is the energy of a monomer in the layer adjacent to the surface (see Fig. 2). If we assign the weight x to a single step of the SAW walker, then the weight of a walk having N steps, with P nearest neighbor contacts, M steps on the surface, and K steps in the layer adjacent to the surface, is $x^N v^P w^M t^K$. An arbitrary SAW configuration can be described, following [5], by using the five restricted generating functions (see Fig. 3). For $G^{(r)}(b)$, the generating functions, in terms of the interaction parameters, have the form

$$A^{(r)}(x, v) = \sum_{N, P} \mathcal{A}^{(r)}(N, P) x^N v^P, \quad (2.3)$$

$$B^{(r)}(x, v) = \sum_{N, P} \mathcal{B}^{(r)}(N, P) x^N v^P, \quad (2.4)$$

$$A_1^{(r)}(x, v, w, t) = \sum_{N, P, M, K} \mathcal{A}_1^{(r)}(N, P, M, K) x^N v^P w^M t^K, \quad (2.5)$$

$$A_2^{(r)}(x, v, w, t) = \sum_{N, P, M, K} \mathcal{A}_2^{(r)}(N, P, M, K) x^N v^P w^M t^K, \quad (2.6)$$

$$B_1^{(r)}(x, v, w, t) = \sum_{N, P, M, K} \mathcal{B}_1^{(r)}(N, P, M, K) x^N v^P w^M t^K, \quad (2.7)$$

where the coefficients have the following meanings:

- $\mathcal{A}^{(r)}(N, P)$ is the number of N -step SAWs, lying completely in the bulk, with P nearest neighbor contacts, and entering $G^{(r)}(b)$ through one corner vertex, and leaving it via a second corner vertex,
- $\mathcal{B}^{(r)}(N, P)$ is the number of N -step SAWs, traversing the $G^{(r)}(b)$ twice, in the bulk, with P nearest neighbor contacts,
- $\mathcal{A}_1^{(r)}(N, P, M, K)$ ($\mathcal{A}_2^{(r)}(N, P, M, K)$) is the number of N -step SAWs entering the

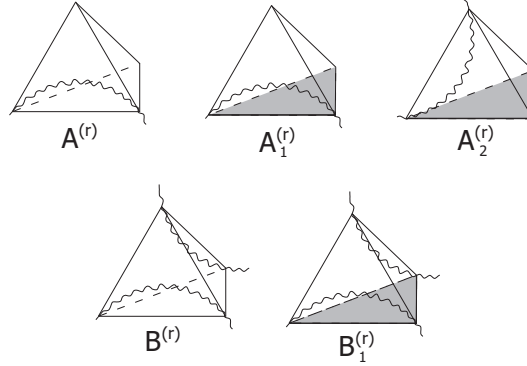


Figure 3. Schematic representation of the five restricted generating functions used in describing all possible polymer configuration within the r th stage 3d SG fractal structure. Thus, for example, $A_1^{(r)}$ represents the SAW paths that start at one tetrahedron vertex that lies on the adsorption wall, and exit at the other vertex that also lies on the adsorption wall. The interior details of the r -th order fractal structure are not shown (they are manifested by the wiggles of the SAW paths).

$G^{(r)}(b)$ through a corner vertex lying on the adsorbing surface, and leaving it via a second corner vertex on the surface (in the bulk, in the case of $\mathcal{A}_2^{(r)}(N, P, M, K)$), with P nearest neighbor contacts, M steps in the surface, and K steps in the layer adjacent to the surface (see Fig. 2), and, finally,

- $\mathcal{B}_1^{(r)}(N, P, M, K)$ is the number of N -step SAWs going twice through the $G^{(r)}(b)$, with P nearest neighbor contacts, M steps in the surface, and K steps in the layer adjacent to the surface.

These generating functions (depicted in Fig. 3) are parameters in the renormalization group (RG) approach, and for any $b \geq 2$, RG equations have the form

$$A^{(r+1)} = \sum_{N_A, N_B} a(N_A, N_B) A^{N_A} B^{N_B}, \quad (2.8)$$

$$B^{(r+1)} = \sum_{N_A, N_B} b(N_A, N_B) A^{N_A} B^{N_B}, \quad (2.9)$$

$$A_1^{(r+1)} = \sum_{N_A, N_B, N_{A_1}, N_{A_2}, N_{B_1}} a_1(N_A, N_B, N_{A_1}, N_{A_2}, N_{B_1}) A^{N_A} B^{N_B} A_1^{N_{A_1}} A_2^{N_{A_2}} B_1^{N_{B_1}}, \quad (2.10)$$

$$A_2^{(r+1)} = \sum_{N_A, N_B, N_{A_1}, N_{A_2}, N_{B_1}} a_2(N_A, N_B, N_{A_1}, N_{A_2}, N_{B_1}) A^{N_A} B^{N_B} A_1^{N_{A_1}} A_2^{N_{A_2}} B_1^{N_{B_1}}, \quad (2.11)$$

$$B_1^{(r+1)} = \sum_{N_A, N_B, N_{A_1}, N_{A_2}, N_{B_1}} b_1(N_A, N_B, N_{A_1}, N_{A_2}, N_{B_1}) A^{N_A} B^{N_B} A_1^{N_{A_1}} A_2^{N_{A_2}} B_1^{N_{B_1}}, \quad (2.12)$$

where we have omitted the superscript (r) on the right-hand side of the above relations. The self-similarity of the fractals under study implies that numbers $a(N_A, N_B)$, $b(N_A, N_B)$, $a_1(N_A, N_B, N_{A_1}, N_{A_2}, N_{B_1})$, $a_2(N_A, N_B, N_{A_1}, N_{A_2}, N_{B_1})$, and $b_1(N_A, N_B, N_{A_1}, N_{A_2}, N_{B_1})$, of the corresponding SAW configurations within the

$G^{(r+1)}(b)$ structure do not depend on r . Starting with the initial conditions

$$\begin{aligned} A^{(0)}(x, v) &= x + 2x^2v + 2x^3v^3, \\ B^{(0)}(x, v) &= x^2v^4, \\ A_1^{(0)}(x, v, w, t) &= wx + (w^2 + t^2)x^2v + 2wt^2x^3v^3, \\ A_2^{(0)}(x, v, w, t) &= tx + 2twx^2v + 2tw^2x^3v^3, \\ B_1^{(0)}(x, v, w, t) &= wtx^2v^4, \end{aligned} \quad (2.13)$$

which correspond to the elementary tetrahedron $G^{(0)}(b)$, one can iterate RG relations (2.8)-(2.12) for various values of interactions v , w and t , and explore the phase diagram. This approach (which implies that interactions are restricted to sites within the elementary tetrahedron $G^{(0)}$ and, moreover, that SAW exits $G^{(r)}$ whenever it reaches its corner vertex [7]) was applied in [5] for 3d $b = 2$ SG fractal. Here we present an analogous type of analysis for the larger b cases.

The average number of monomers in contact with the adsorption wall, for SAW spanning a $G^{(r)}(b)$ can be expressed in terms of the partial derivatives of the generating functions $A_1^{(r)}$ and $A_2^{(r)}$:

$$\begin{aligned} \langle M^{(r)} \rangle &= \frac{\sum_{N,P,M,K} M \left(\mathcal{A}_1^{(r)}(N, P, M, K) + \mathcal{A}_2^{(r)}(N, P, M, K) \right) x^N v^P w^M t^K}{A_1^{(r)} + A_2^{(r)}} \\ &= \frac{w}{A_1^{(r)} + A_2^{(r)}} \left(\frac{\partial A_1^{(r)}}{\partial w} + \frac{\partial A_2^{(r)}}{\partial w} \right) = \frac{w}{A_1^{(r)} + A_2^{(r)}} \left(A_{1,w}^{(r)} + A_{2,w}^{(r)} \right), \end{aligned} \quad (2.14)$$

whereas the total average number of monomers can be expressed in the form

$$\begin{aligned} \langle N^{(r)} \rangle &= \frac{\sum_{N,P,M,K} N \left(\mathcal{A}_1^{(r)}(N, P, M, K) + \mathcal{A}_2^{(r)}(N, P, M, K) \right) x^N v^P w^M t^K}{A_1^{(r)} + A_2^{(r)}} \\ &= \frac{x}{A_1^{(r)} + A_2^{(r)}} \left(\frac{\partial A_1^{(r)}}{\partial x} + \frac{\partial A_2^{(r)}}{\partial x} \right) = \frac{x}{A_1^{(r)} + A_2^{(r)}} \left(A_{1,x}^{(r)} + A_{2,x}^{(r)} \right). \end{aligned} \quad (2.15)$$

From the RG equations (2.8)-(2.12) one can obtain recursion relations for the derivatives of the generating functions in the following matrix form

$$\begin{pmatrix} A'_{1,w} \\ A'_{2,w} \\ B'_{1,w} \end{pmatrix} = \mathbf{R}_S \begin{pmatrix} A_{1,w} \\ A_{2,w} \\ B_{1,w} \end{pmatrix}, \quad \begin{pmatrix} A'_x \\ B'_x \\ A'_{1,x} \\ A'_{2,x} \\ B'_{1,x} \end{pmatrix} = \mathbf{R} \begin{pmatrix} A_x \\ B_x \\ A_{1,x} \\ A_{2,x} \\ B_{1,x} \end{pmatrix}, \quad (2.16)$$

where matrices \mathbf{R}_S and \mathbf{R} are comprised of partial derivatives of generating functions A' , B' , A'_1 , A'_2 and B'_1 , corresponding to SAWs spanning the generator $G^{(r+1)}(b)$, in respect to generating functions A , B , A_1 , A_2 and B_1 , corresponding to $G^{(r)}(b)$:

$$\mathbf{R}_S = \begin{pmatrix} \frac{\partial A'_1}{\partial A_1} & \frac{\partial A'_1}{\partial A_2} & \frac{\partial A'_1}{\partial B_1} \\ \frac{\partial A'_2}{\partial A_1} & \frac{\partial A'_2}{\partial A_2} & \frac{\partial A'_2}{\partial B_1} \\ \frac{\partial B'_1}{\partial A_1} & \frac{\partial B'_1}{\partial A_2} & \frac{\partial B'_1}{\partial B_1} \end{pmatrix}, \quad \mathbf{R} = \begin{pmatrix} \frac{\partial A'}{\partial A} & \frac{\partial A'}{\partial B} & 0 & 0 & 0 \\ \frac{\partial B'}{\partial A} & \frac{\partial B'}{\partial B} & 0 & 0 & 0 \\ \frac{\partial A'_1}{\partial A} & \frac{\partial A'_1}{\partial B} & \frac{\partial A'_1}{\partial A_1} & \frac{\partial A'_1}{\partial A_2} & \frac{\partial A'_1}{\partial B_1} \\ \frac{\partial A'_2}{\partial A} & \frac{\partial A'_2}{\partial B} & \frac{\partial A'_2}{\partial A_1} & \frac{\partial A'_2}{\partial A_2} & \frac{\partial A'_2}{\partial B_1} \\ \frac{\partial B'_1}{\partial A} & \frac{\partial B'_1}{\partial B} & \frac{\partial B'_1}{\partial A_1} & \frac{\partial B'_1}{\partial A_2} & \frac{\partial B'_1}{\partial B_1} \end{pmatrix}.$$

Starting with the initial conditions for the derivatives

$$\begin{aligned}
\frac{\partial A^{(0)}}{\partial x} &= 1 + 2xv + 6x^2v^3, & \frac{\partial B^{(0)}}{\partial x} &= 2xv^4, \\
\frac{\partial A_1^{(0)}}{\partial x} &= w + 2(w^2 + t^2)xv + 6wt^2x^2v^3, & \frac{\partial A_2^{(0)}}{\partial x} &= t + 4twxv + 6tw^2x^2v^3, \\
\frac{\partial B_1^{(0)}}{\partial x} &= 2wt xv^4, & \frac{\partial A_1^{(0)}}{\partial w} &= x + 2wx^2v + 2t^2x^3v^3, \\
\frac{\partial A_2^{(0)}}{\partial w} &= 2tvx^2 + 4twx^3v^3, & \frac{\partial B_1^{(0)}}{\partial w} &= tx^2v^4
\end{aligned} \tag{2.17}$$

and iterating recursion equations (2.16), it is possible to establish the relation between the average number of adsorbed monomers $\langle M^{(r)} \rangle$ (2.14) and the average length of the polymer chain $\langle N^{(r)} \rangle$ (2.15) in the limit $r \rightarrow \infty$, for various values of the interaction parameters v, w , and t .

3. Exact approach: phase diagram and critical exponents

To solve exactly the adsorption problem of a self-interacting SAW for arbitrary member (for any $b \geq 2$) of the 3d SG family, it is necessary to find all coefficients that appear in the set (2.8)–(2.12) of the RG equations. The $b = 2$ case has been completely analyzed in [5], while in the $b = 3$ and $b = 4$ cases only the bulk RG equations (2.8) and (2.9) have been studied, in [6] and [8] respectively. In this paper we make a complete analysis of the $b = 3$ and $b = 4$ cases, that is, including the adsorption RG equations (2.10)–(2.12).

3.1. The $b = 3$ SG fractal

The RG equations (2.8) and (2.9) for the bulk parameters A and B , found in [6] for the case of the $b = 3$ SG fractal, have the form

$$\begin{aligned}
A^{(r+1)} &= A^3 + 6A^4 + 16A^5 + 34A^6 + 76A^7 + 112A^8 + 112A^9 + 64A^{10} + 8A^4B + \\
&36A^5B + 140A^6B + 292A^7B + 424A^8B + 332A^9B + 12A^3B^2 + 12A^4B^2 + \\
&118A^5B^2 + 380A^6B^2 + 806A^7B^2 + 664A^8B^2 + 72A^4B^3 + 352A^5B^3 + \\
&704A^6B^3 + 1728A^7B^3 + 344A^4B^4 + 1568A^5B^4 + 848A^6B^4 + \\
&264A^4B^5 + 3192A^5B^5 + 320A^3B^6,
\end{aligned} \tag{3.1}$$

$$\begin{aligned}
B^{(r+1)} &= A^6 + 12A^7 + 40A^8 + 60A^9 + 32A^{10} + 28A^6B + 88A^7B + 224A^8B + \\
&160A^9B + 40A^6B^2 + 496A^7B^2 + 596A^8B^2 + 176A^5B^3 + 768A^6B^3 + \\
&1056A^7B^3 + 88A^3B^4 + 264A^5B^4 + 2534A^6B^4 + 1152A^4B^5 + \\
&1888A^5B^5 + 5808A^4B^6 + 1936A^3B^7 + 4308A^2B^8.
\end{aligned} \tag{3.2}$$

Here we give a summary of the analysis of the above set of equations. For small values of the monomer–monomer interaction ($v < v_\theta$), the extended SAW phase fixed point $(A_E, B_E) = (0.34196, 0.02395)$ is reached through the RG transformations.

Linearization of the RG equations in the vicinity of this fixed point gives only one relevant eigenvalue $\lambda_\nu^E = 5.36201$. The mean-squared end-to-end distance $\langle R_N^2 \rangle$ of the N -step polymer chain, in general case, behaves asymptotically (for $N \gg 1$) as

$$\langle R_N^2 \rangle \sim N^{2\nu}, \quad (3.3)$$

where the critical exponent ν is given by

$$\nu = \frac{\ln b}{\ln \lambda_\nu}, \quad (3.4)$$

which for $b = 3$ gives $\nu_E = 0.6542$. Starting with $v = v_\theta$, the RG equations lead to the fixed point $(A_\theta, B_\theta) = (0.20717, 0.43075)$, for which both eigenvalues $\lambda_\nu^\theta = 8.72308$ and $\lambda_\alpha^\theta = 2.45012$ are relevant. At this fixed point critical exponent $\nu_\theta = \ln 3 / \ln \lambda_\nu^\theta = 0.5072$ is smaller than ν_E , which is the manifestation of the so-called collapse transition. At the collapse transition, the free energy per site f behaves as

$$f \sim |v - v_\theta|^{2-\alpha}, \quad (3.5)$$

where the critical exponent α in general case is given by

$$\alpha = 2 - \frac{\ln \lambda_\nu^\theta}{\ln \lambda_\alpha^\theta}, \quad (3.6)$$

and in this specific case it is negative, $\alpha = -0.4170$. Depending on the value of the one-step weight (fugacity) x , for strong monomer-monomer interactions ($v > v_\theta$) RG equations (3.1) and (3.2) bring about the trivial fixed point $(A, B)^* = (0, 0)$, for $x < x^*(v)$, or $(A, B)^* = (\infty, \infty)$ for $x > x^*(v)$, whereas for x precisely equal to $x^*(v)$, the fixed point $(A_G, B_G) = (0, \infty)$ is reached. Analyzing the RG equations in the vicinity of (A_G, B_G) , by keeping only the dominant terms in the right-hand side of (3.1) and (3.2), one can find $\nu_G = 0.48195$. Since the fractal dimension $d_f^{\text{poly}} = 1/\nu_G = 2.07491$ of the SAW in this case is larger than the fractal dimension of the extended SAW (for $v \leq v_\theta$), but still less than the fractal dimension of the underlying lattice $d_f = 2.09590$ one can conclude that fixed point $(0, \infty)$ corresponds to the 'semi-compact' phase [6]. This finding is in contrast with the results obtained for polymers on homogeneous lattices and on the $b = 2$ 3d SG fractal lattice [7], where one finds $d_f^{\text{poly}} = d_f$.

In order to establish the specific form of the complete set of the exact RG equations (2.8)–(2.12), required for the study of the adsorption problem on the $b = 3$ SG fractal, we have enumerated the requisite SAW configurations, achieving thereby the pertinent RG coefficients. This procedure is rather complex, as well as the corresponding set of coefficients, and for this reason we give them in the Appendix A. The physical picture that follows from these RG equations, for various values of the interaction parameters (v, t and w), is unusually rich and we present it in what follows.

Numerical study of the adsorption RG equations (given in the Appendix A) shows that for $w > 1$ (attractive surface) an unbinding transition appears at a finite temperature only if $t < 1$ (repulsive interaction in the layer adjacent to the surface). The nature of this transition depends on the value of the monomer-monomer interaction v . This situation is analogous to the previously studied cases of the two-dimensional

and three-dimensional $b = 2$ Sierpinski gasket fractals [5], but the new physical features do appear.

3.1.1. Extended SAW phase For the chosen initial conditions (2.13) we found the critical value of monomer–monomer interactions $v_\theta = 2.446161$ (which is different from the value found in [6], because of the slightly different initial conditions, but which does not affect the overall critical behavior). For weak monomer–monomer interactions $v < v_\theta$, and the corresponding critical fugacity $x = x^*(v)$, RG equations (3.1) and (3.2) for the bulk parameters A and B iterate towards the fixed point (A_E, B_E) .

Behavior of surface RG parameters $(A_1^{(r)}, A_2^{(r)}, B_1^{(r)})$ depends primarily on the corresponding interaction parameter w . Thus, for weak interactions $w < w_c(t, v)$, and $x = x^*(v)$, the parameters $(A_1^{(r)}, A_2^{(r)}, B_1^{(r)})$ tend to $(0, 0, 0)$, when $r \rightarrow \infty$, which indicates that polymer, being in the extended coil phase, stays away from the attractive surface. We shall refer to this state as the desorbed extended (DE) phase, determined by the RG fixed point

$$(A, B, A_1, A_2, B_1)^* = (A_E, B_E, 0, 0, 0). \quad (3.7)$$

This behavior changes abruptly at $w = w_c(t, v)$, where $A_1^{(r)}, A_2^{(r)} \rightarrow A_E$ and $B_1^{(r)} \rightarrow B_E$. The new behavior is described by the new fixed point

$$(A, B, A_1, A_2, B_1)^* = (A_E, B_E, A_E, A_E, B_E), \quad (3.8)$$

which is the symmetric special fixed point, that corresponds to the unbinding transition of the SAW. If w is increased beyond $w_c(t, v)$, and for the fugacity equal to $x = x^*(v)$, bulk parameters still approach (A_E, B_E) , but the surface RG parameters diverge, implying that critical fugacity x_c is smaller than $x^*(v)$. A thorough analysis shows that x_c depends on the values of v, w , and t , whereas RG parameters flow towards the new fixed point

$$(A, B, A_1, A_2, B_1)^* = (0, 0, A_E^{2d}, 0, 0), \quad (3.9)$$

where $A_E^{2d} = 0.551147$ is the fixed point for the $b = 3$ two-dimensional SG fractal (see [9]), meaning that for strongly attractive surface polymer remains adsorbed (this is the adsorbed SAW phase).

At the symmetric special fixed point (3.8) linearized RG equations have two relevant eigenvalues: the larger $\lambda_\nu^E = 5.36201$, already found for the bulk RG equations, and the smaller $\lambda_S^E = 3.32923$. The matrix of the linearized RG equations is equal to the matrix \mathbf{R} in (2.16), which means that

$$\langle N^{(r)} \rangle \sim (\lambda_\nu^E)^r, \quad \text{for } r \gg 1, \quad (3.10)$$

whereas the largest eigenvalue of the matrix \mathbf{R}_S in (2.16) is equal to λ_S^E , meaning that

$$\langle M^{(r)} \rangle \sim (\lambda_S^E)^r, \quad \text{for } r \gg 1. \quad (3.11)$$

Consequently, for $r \rightarrow \infty$, it follows

$$\langle M^{(r)} \rangle \sim \langle N^{(r)} \rangle^\phi, \quad (3.12)$$

where the crossover exponent ϕ is equal to

$$\phi_E = \frac{\ln \lambda_S^E}{\ln \lambda_\nu^E} = 0.7162. \quad (3.13)$$

This completes our analysis of the extended polymer phase.

3.1.2. θ -line ($v = v_\theta$) Here we organize our discussion of various phases that appear along the θ -line in the phase space (v, w) , for $v = v_\theta = 2.446161$ and for various values of w .

For $x = x^*(v_\theta) = 0.109683$ and $w < w_\theta(t)$, RG iterations lead to the fixed point

$$(A, B, A_1, A_2, B_1)^* = (A_\theta, B_\theta, 0, 0, 0), \quad (3.14)$$

which means that for small values of w polymer remains desorbed, in the solution, in the form of the θ -chain. On the other hand, for $w > w_\theta(t)$ critical fugacity $x_c(v_\theta, w, t)$ is less than $x^*(v_\theta)$, and the relevant fixed point is again $(0, 0, A_E^{2d}, 0, 0)$ which describes an adsorbed two-dimensional SAW (as in the case $v < v_\theta$).

At the critical value $w = w_\theta(t)$, and x still equal to $x^*(v_\theta)$, RG parameters flow towards the new fixed point

$$(A, B, A_1, A_2, B_1)^* = (A_\theta, B_\theta, A_{1\theta}, A_{2\theta}, B_{1\theta}), \quad (3.15)$$

whose coordinates $A_{1\theta}, A_{2\theta}$, and $B_{1\theta}$ depends on the value of t , and accordingly there are five possible situations that should be analyzed.

First, for $0 \leq t < t_1^* = 0.1553901$, the new fixed point is

$$(A, B, A_1, A_2, B_1)^* = (A_\theta, B_\theta, A_E^{2d}, 0, 0), \quad (3.16)$$

that controls the coexistence between the θ -chain in the bulk and the adsorbed two-dimensional SAW.

Second, we find the fixed point

$$(A, B, A_1, A_2, B_1)^* = (A_\theta, B_\theta, 0.5234, 0.1637, 0.0305), \quad (3.17)$$

for the critical value of the interaction $t = t_1^*$, with four eigenvalues larger than one — the two bulk values λ_ν^θ and λ_α^θ , and the two surface eigenvalues $\lambda_{S1}^\theta = 3.96291$, and $\lambda_{S2}^\theta = 1.28383$, which brings about

$$\phi_\theta = \frac{\ln \lambda_{S1}^\theta}{\ln \lambda_\nu^\theta} = 0.6357. \quad (3.18)$$

Third, in the interval between the two critical values of the interaction parameter t , $t_1^* < t < t_2^* = 0.6573781$, the new fixed point is

$$(A, B, A_1, A_2, B_1)^* = (A_\theta, B_\theta, 0.19265, 0.44713, 0.132446), \quad (3.19)$$

for which, in addition to the relevant bulk eigenvalues, there is only one surface relevant eigenvalue $\lambda_S^\theta = 3.663797$, and the crossover exponent is equal to

$$\phi_\theta = \frac{\ln \lambda_S^\theta}{\ln \lambda_\nu^\theta} = 0.5995. \quad (3.20)$$

Fourth, for the second critical t_2^* , the RG parameters flow towards the symmetric fixed point

$$(A, B, A_1, A_2, B_1)^* = (A_\theta, B_\theta, A_\theta, A_\theta, B_\theta), \quad (3.21)$$

where, as in the case of the first critical value t_1^* , one finds two relevant surface eigenvalues $\lambda_{S1}^\theta = 5.368208$ and $\lambda_{S2}^\theta = 1.718244$, wherefrom one obtains the crossover exponent

$$\phi_\theta = \frac{\ln \lambda_{S1}^\theta}{\ln \lambda_\nu^\theta} = 0.7758. \quad (3.22)$$

Fifth, for $t_2^* < t < 1$ the following fixed point

$$(A, B, A_1, A_2, B_1)^* = (A_\theta, B_\theta, 0, 0, \infty) \quad (3.23)$$

is reached. By keeping the dominant terms on the right-hand side of the RG equations (A.1–A.3), for the surface parameters A_1, A_2 , and B_1 (see Appendix A), the RG equations attain the approximate form

$$\begin{aligned} A_1' &\approx (128A_\theta^2 + 124A_\theta^3 + 292A_\theta^4 + 264A_\theta^2B_\theta + 944A_\theta^3B_\theta + 320A_\theta B_\theta^2)A_1^2B_1^4 = c_1A_1^2B_1^4, \\ B_1' &\approx (472A_\theta^4 + 1452A_\theta^3B_\theta + 1452A_\theta^2B_\theta^2 + 4308A_\theta B_\theta^3)A_1B_1^5 = c_2A_1B_1^5, \\ A_2' &\approx c_3A_2, \end{aligned} \quad (3.24)$$

where $c_1 \approx 6.26$, $c_2 \approx 89.32$, and $c_3 \approx 0.127$. Introducing the new variable $y_1 = B_1A_1^{1/4}$ we obtain the tractable form of the approximate RG equations

$$A_1' = c_1y_1^4A_1, \quad y_1' = c_1^{1/4}c_2y_1^6, \quad A_2' = c_3A_2, \quad (3.25)$$

which have the fixed point $(0, 0, y_1^* = c_1^{-1/20}c_2^{-1/5})$. Linearizing these RG equations in the vicinity of the fixed point, one relevant eigenvalue $\lambda_S^\theta = 6$ is found, with the corresponding crossover exponent ϕ_θ

$$\phi_\theta = \frac{\ln \lambda_S^\theta}{\ln \lambda_\nu^\theta} = 0.8272. \quad (3.26)$$

3.1.3. Semi-compact regime ($v > v_\theta$) For values of the monomer–monomer interaction parameter v larger than v_θ , and for the fugacity x equal to the bulk critical value $x^*(v)$, the bulk RG parameters (A, B) flow towards $(0, \infty)$, while critical behavior of the surface RG parameters (A_1, A_2, B_1) depends on the values of both surface interaction parameters w and t . In particular, for any value of t between 0 and 1, there is a critical value $w_c(t, v)$ such that (A_1, A_2, B_1) flows towards $(0, 0, 0)$, for $w < w_c(t, v)$, whereas for w precisely equal to $w_c(t, v)$ one observes

$$(A, B, A_1, A_2, B_1) \rightarrow \begin{cases} (0, \infty, A_{SAW}^{2d}, 0, 0), & v_\theta < v < v_\theta + \epsilon \\ (0, \infty, 0, 0, \infty), & v > v_\theta + \epsilon \end{cases} \quad (3.27)$$

for $t < t^* \approx 0.156$, and

$$(A, B, A_1, A_2, B_1) \rightarrow (0, \infty, 0, 0, \infty), \quad (3.28)$$

for $t > t^*$ and all $v > v_\theta$.

The fixed points $(0, \infty, 0, 0, 0)$, $(0, \infty, A_{SAW}^{2d}, 0, 0)$, and $(0, \infty, 0, 0, \infty)$, correspond to the desorbed semi-compact polymer chain (globule), to the coexistence between

the globule in the bulk and the adsorbed 2d polymer, and to the adsorbed globule, respectively. Finally, for values of the parameter w larger than the critical value $w_c(t, v)$, the critical fugacity $x_c = x^*(v, w, t)$ is smaller than its bulk critical value $x^*(v)$, and RG parameters iterate towards the fixed point $(0, 0, A_{SAW}^{2d}, 0, 0)$, which corresponds to the fully adsorbed polymer.

The adsorbed globule phase can be analyzed by keeping the dominant terms on the right-hand side of the RG equations (3.1), (3.2), and (A.1)–(A.3), in the vicinity of the fixed point $(0, \infty, 0, 0, \infty)$. Accordingly, one can obtain the following approximate equations:

$$\begin{aligned} A' &\approx 320A^3B^6, & B' &\approx 4308A^2B^8, & A_1' &\approx 320AA_1^2B^2B_1^4, \\ A_2' &\approx 44AA_1^3BB_1^3, & B_1' &\approx 4308AA_1B^3B_1^5. \end{aligned} \quad (3.29)$$

Introducing new variables

$$y = AB^z, \quad y_1 = A_1/A, \quad y_2 = A^q/A_2, \quad y_3 = B_1A^z, \quad (3.30)$$

where

$$z = \frac{\sqrt{73} - 5}{12}, \quad q = \frac{19 + \sqrt{73}}{12}, \quad (3.31)$$

equations (3.29) transform into more tractable form

$$A' = 320A^{3-z}y^6, \quad y' = 320^z 4308 y^{8+6z}, \quad (3.32)$$

$$y_1' = \frac{y_1^2 y_3^4}{y^4}, \quad y_3' = 320^z 4308 y_1 y^{6z+3} y_3^5, \quad (3.33)$$

$$y_2' = \frac{320^q y^{6q-1}}{44 y_1^3 y_3^3}. \quad (3.34)$$

The new equations (3.32) have fixed point $A^* = 0$, $y^* = (4308 \times 320^z)^{-1/(7+6z)}$, with one relevant bulk eigenvalue $\lambda_\nu^G = 8+6z = (11+\sqrt{73})/2$ (see [6]). Inserting y^* into equations (3.33) one finds that corresponding equations for the fixed point (y_1^*, y_3^*) are mutually linearly dependent. More precisely, the only fact that springs from these equations is the relation

$$y^* = (y_1^*)^{1/4} y_3^*. \quad (3.35)$$

For various values of t , large enough v and corresponding bulk critical fugacity $x^*(v)$, and the critical value $w_c(t, v)$, point (y_1, y_3) tends to different fixed points (y_1^*, y_3^*) , but the above relation stays satisfied. Obviously, knowing (y_1^*, y_3^*) , from equation (3.34) one can calculate the fixed value y_2^* , which is also different for various t and v , but on the other hand is in excellent agreement with the value obtained via explicit iteration of the expression A^q/A_2 .

Linearizing equations (3.33), (3.34) around the corresponding fixed point (y_1^*, y_2^*, y_3^*) the second relevant eigenvalue $\lambda_S^G = 6$ is found, so that the crossover exponent ϕ is equal to

$$\phi_G = \frac{\ln 6}{\ln\left(\frac{11+\sqrt{73}}{2}\right)} = 0.786. \quad (3.36)$$

This result is in agreement with the value estimated via direct numerical analysis, performed using equations (2.14) and (2.15), as explained in Section 2. One should also observe that obtained value of ϕ_G is slightly larger than $d_f^{2d}/d_f^{3d} = 0.7781$, which has been predicted in [5] for SAW in the compact phase. Of course, due to the topological frustration, SAW on 3d $b = 3$ Sierpinski fractal lattice can not, even for large monomer—monomer interaction, have a compact configuration (see [6]). Instead, it is in the semi-compact phase, in which its fractal dimension is less than the fractal dimension of the lattice (although larger than fractal dimension of SAW for $v \leq v_\theta$).

3.2. 3d $b = 4$ SG fractal

As the scaling parameter b increases the number of possible polymer configurations on the 3d SG fractal lattices quickly grows. The RG equations, for $b = 4$, for the bulk RG parameters A and B have been found and analyzed by Maričić and Elezović–Hadžić (see [8] and Appendix B). The conclusion has been reached that qualitatively the physical picture of the polymer behavior in the bulk, for $b = 4$, is similar to the cases $b = 2$ and $b = 3$. There are three possible phases in which polymer can reside, which we review in the following paragraph.

For small values of the monomer–monomer interaction $v < v_\theta = 2.33187$ polymer is in the swollen state. The fixed point $(A, B)^* = (A_E, B_E) = (0.2899, 0.0122)$ is reached for any $v < v_\theta$ and for the corresponding critical fugacity $x = x^*(v)$. Linearizing RG equations around this fixed point one gets single relevant eigenvalue $\lambda_\nu^E = 8.6924$, and the concomitant critical exponent ν is equal to $\nu_E = \ln b / \ln \lambda_\nu^E = 0.6410$. On the other hand, the low-temperature fixed point $(A, B)^* = (A_G, B_G) = (0, 22^{-1/3})$ is reached when the RG iteration starts with $v > v_\theta$. In this case, there is one relevant eigenvalue $\lambda_\nu^G = 16$, and the end-to-end critical exponent is $\nu_G = 1/2$. The fractal dimension of the chain $d_f^{\text{poly}} = 1/\nu_G = 2$ is less than the fractal dimension of the lattice $d_f = \ln 20 / \ln 4 \approx 2.16$. This means that polymer is in the semi-compact phase for strong monomer–monomer interactions, as in the $b = 3$ case, and in contrast with the cases of polymer on the $b = 2$ fractal and on the Euclidean lattices. Finally, when $v = v_\theta$, the tricritical fixed point $(A, B)^* = (A_\theta, B_\theta) = (0.1929, 0.3388)$, that corresponds to the collapse transition, is reached. In this case there are two relevant eigenvalues, $\lambda_\nu^\theta = 15.4230$ and $\lambda_\alpha^\theta = 5.5357$. Consequently, the critical exponent ν is equal to $\nu_\theta = \ln b / \ln \lambda_\nu^\theta = 0.5067$. In addition, we have obtained the specific heat critical exponent $\alpha = 0.4012 > 0$ which reveals the singular behavior, which was observed in the case $b = 2$ but not in the case $b = 3$.

Recursion relations for the surface RG parameters A_1 , A_2 , and B_1 are cumbersome (each of the corresponding equations has more than 3000 terms) and we are not going to quote them here (but they are available upon the request to the authors). Detailed numerical analysis of these RG equations shows that, depending on the value of interaction parameters v , w , and t , the following phases and the corresponding fixed points are accessible:

- extended desorbed phase, $(A_E, B_E, 0, 0, 0)$, for $v < v_\theta$ and $w < w_c(t, v)$,
- semi-compact desorbed phase, $(0, B_G, 0, 0, 0)$, for $v > v_\theta$ and $w < w_c(t, v)$,
- desorbed θ -chain, $(A_\theta, B_\theta, 0, 0, 0)$, for $v = v_\theta$ and $w < w_\theta(t)$,
- fully adsorbed chain, $(0, 0, A_{SAW}^{2d}, 0, 0)$, for $w > w_c(t, v)$, where $A_{SAW}^{2d} = 0.5063$ is the fixed point for the 2d $b = 4$ SG fractal (see [9]),
- coexistence of the globule in the bulk and the 2d adsorbed polymer chain, $(0, B_G, A_E^{2d}, 0, 0)$, for $v_\theta < v < v_\theta + \epsilon$ (where ϵ is a small positive number whose specific value depends on t) and $w = w_c(t, v)$,
- surface attached extended chain, special symmetric fixed point, $(A_E, B_E, A_E, A_E, B_E)$, for $v < v_\theta$ and $w = w_c(t, v)$, with the relevant eigenvalues λ_ν^E and $\lambda_S^E = 4.4533$ that give the crossover exponent $\phi_E = \ln \lambda_S^E / \ln \lambda_\nu^E = 0.6907$,
- surface attached globule, $(0, B_G, 0, 0, B_G)$, for $v > v_\theta + \epsilon$ and $w = w_c(t, v)$, with the relevant eigenvalues λ_ν^G and $\lambda_S^G = 9$ and $\phi_G = 0.7924$,
- surface attached θ -chain, multi-critical point $(A_\theta, B_\theta, A_{1\theta}, A_{2\theta}, B_{1\theta})$, for $v = v_\theta$ and $w = w_\theta(t)$, with

$$(A_{1\theta}, A_{2\theta}, B_{1\theta}) = \begin{cases} (0.2275, 0.3659, 0.0433), & t < t^* \\ (A_\theta, A_\theta, B_\theta), & t = t^* = 0.9577 \\ (0, 0, 0.3643), & t^* < t < 1 \end{cases} \quad (3.37)$$

for which one finds

$$\lambda_S^\theta = \begin{cases} 4.9036, & t < t^* \\ 8.4078, & t = t^* \\ 9, & t^* < t < 1 \end{cases} \quad \text{and} \quad \phi_\theta = \begin{cases} 0.5811, & t < t^* \\ 0.7782, & t = t^* \\ 0.8031, & t^* < t < 1 \end{cases} \quad (3.38)$$

In the last part of this section we summarize, in Table 1, the numerical results obtained via the exact RG approach, for the 3d SG fractals $b = 2, 3, 4$, and provide the relevant discussion of the pertinent phase diagrams. One should notice that we first give the fixed point values of the bulk parameters A^* and B^* and the accompanying end-to-end critical exponent ν . For each b there are three fixed points, which correspond to the three bulk phases — the extended polymer phase, the θ -chain phase, and the globular (collapsed) phase. Furthermore, for a given b , one may observe that A^* decreases, while B^* increases, with increasing of the monomer-monomer interaction v , and consequently ν decreases. On the other hand, when b increases ν decreases for the extended phase and the θ -chain phase, whereas in the case of the globular phase ν does not display a monotonic behavior. Besides, in the globular phase, for $b = 3$ and $b = 4$ the exponent ν is larger than the reciprocal of the fractal dimension of the underlying lattices, which implies that the globular phase is not compact. This is in contrast with the $b = 2$ case (as well as, in contrast with the Euclidean lattices), where $\nu = 1/d_f$.

In Table 1 we also give the fixed point values of the surface RG parameters A_1^*, A_2^*, B_1^* and the corresponding values of the crossover exponent ϕ , for the unbinding transitions from adsorbed polymer phase to various desorbed phases. The relevant phase diagram is given in Fig. 4, for the $b = 3$ SG fractal (a similar phase diagram for $b = 2$

Table 1. Fixed points and critical exponents ν and ϕ for different self-avoiding walk phases on 3d Sierpinski fractals, obtained via exact renormalization group approach. Values for the bulk fixed point (A^*, B^*) and the critical exponent ν for $b = 2$ and 3 fractals were obtained in [7] and [6] respectively, whereas the surface bulk point (A_1^*, A_2^*, B_1^*) and the crossover exponent ϕ were previously known for the $b = 2$ fractal only [5].

extended chain phase							
b	A^*	B^*	ν_E	A_1^*	A_2^*	B_1^*	ϕ_E
2	0.4294	0.0499	0.6740	0.4294	0.4294	0.0499	0.7481
3	0.3491	0.0239	0.6542	0.3491	0.3491	0.0239	0.7162
4	0.2899	0.0122	0.6411	0.2899	0.2899	0.0122	0.6907
θ -chain							
b	A^*	B^*	ν_θ	A_1^*	A_2^*	B_1^*	ϕ_θ
2	1/3	1/3	0.5923	0.4477	0.4528	0.0815	0.6264
3	0.2071	0.4307	0.5072	0.5234	0.1637	0.0305	0.6357
				0.1926	0.4471	0.1324	0.5995
				0.2071	0.2071	0.4307	0.7758
				0	0	∞	0.8272
4	0.1929	0.3388	0.5067	0.2275	0.3659	0.0433	0.5811
				0.1929	0.1929	0.3388	0.7782
				0	0	0.3643	0.8301
globular phase							
b	A^*	B^*	ν_G	A_1^*	A_2^*	B_1^*	ϕ_G
2	0	$22^{-1/3}$	1/2	0	0	$22^{-1/3}$	0.7925
3	0	∞	0.4819	0	0	∞	0.7860
4	0	$22^{-1/3}$	1/2	0	0	$22^{-1/3}$	0.7925

was obtained in [5], whereas in the course of this work we obtained a diagram, of the same type, for $b = 4$). In Fig. 4, the unbinding transitions are represented by the curve that separates the “adsorbed chain” region from the “desorbed chain” regions. On this curve lies the multi-critical point, so that the part of the curve for smaller values of the parameter v ($v < v_\theta$) corresponds to the extended attached chain phase, while for larger values of v ($v > v_\theta$) the curve corresponds to the attached semi-compact phase. The fixed point that defines the extended attached chain phase is a symmetric special fixed point, that is, $A_1^* = A_2^* = A^*$ and $B_1^* = B^*$, with the corresponding crossover exponent which decreases with increasing of the scaling parameter b (see the top part of the Table 1). Here we would like to mention that this behavior of the crossover exponent will be demonstrated for larger b as well, using the MCRG method (see the next section of this paper).

Continuing our discussion guided by the results presented in Table 1, we focus now on the attached globular phase ($v > v_\theta$). For this phase, the fixed point parameters

satisfy the relations $A_1^* = A_2^* = A^* = 0$ and $B_1^* = B^*$, where $B^* = 22^{-1/3}$ for $b = 2$ and $b = 4$, while $B^* = \infty$ for $b = 3$. It is interesting to observe that the critical exponents ν and ϕ are the same for the fractals with $b = 2$ and $b = 4$, while for $b = 3$ these two exponents are somewhat smaller. Besides, we should point out that only for $b = 2$ the crossover exponent ϕ is equal to the ratio d_f^{2d}/d_f^{3d} which is related to the fact that only for $b = 2$ the globular phase is compact. Finally, by comparing values of the crossover exponent ϕ , we may observe that in the attached globular phase the number of adsorbed monomers is relatively larger than in the corresponding Euclidean phases ($\phi = 2/3$).

Results obtained for the multi-critical points for the fractals with $b = 3$ and $b = 4$ (see the middle right part of Table I) appear to be dependent on the parameter t that describes energy of a monomer in the layer adjacent to the adsorbing boundary. This is manifested by several possible fixed points, in contrast to the case $b = 2$. Particularly, the position of the multi-critical point, as well as the shape of the critical line $w_c(v)$ (that separates the adsorbed phase from the desorbed phases), depend on the particular value of t (see Fig. 4). For the case $b = 3$ there are four fixed points that correspond to the surface attached θ -chain, two of which (the first and the third one) appear to be very repulsive (each with four eigenvalues larger than one) and can be approached for the critical values $t_1^* = 0.1553$ and $t_2^* = 0.6573$ of the parameter t . The latter fixed point appears to be symmetric ($A_1^* = A_2^* = A^* = A_\theta$ and $B_1^* = B^* = B_\theta$) and accordingly is the only point that describes the isotropic chain. The other two fixed points, the second and the fourth, are less repulsive (each of them has three eigenvalues larger than one), and can be reached for any value of the parameter t in the intervals $t_1^* < t < t_2^*$ and $t_2^* < t < 1$, respectively.

Contrary to the expectation, that may be formed on the findings presented for the cases $b = 2$ and $b = 3$, that number of attainable multi-critical points will continue to increase with increasing b , in the $b = 4$ case only three multi-critical points can be reached. Indeed, for $b = 4$ there is only one critical value $t^* = 0.9577$ of the parameter t such that for $0 < t < t^*$ and for $1 > t > t^*$, two different nonsymmetric fixed points (one for each of the two intervals) with three eigenvalues larger than one are reached. On the other hand, highly repulsive symmetric point, with four eigenvalues larger than one, can be approached only for $t = t^*$. Each one of the three multi-critical points describes its pertinent surface attached θ -chain which is manifested by the facts that $A_2^* > A_1^* > A^* = A_\theta$ and $B_1^* < B_\theta$ for $t < t^*$, $A_1^* = A_2^* = 0$ and $B_1^* < B_\theta$ for $t > t^*$, meaning that the corresponding two phases are anisotropic, whereas for the critical value $t = t^*$ the surface attached θ -chain is isotropic. Finally, one can notice that crossover exponent ϕ increases with t (which was not the case for $b = 3$), and moreover that the particular values of ϕ for $b = 3$ and $b = 4$, in their relevant intervals $1 > t \geq t_2^*$ and $1 > t \geq t^*$, are rather close.

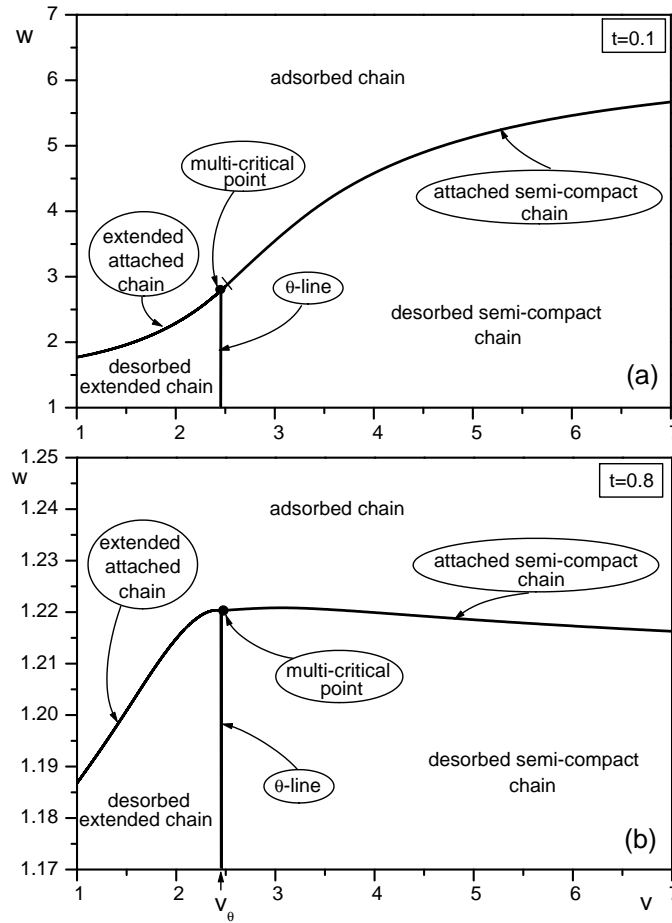


Figure 4. Phase diagram in the case of the $b = 3$ SG fractal for two different values of the interaction parameter t : (a) $t = 0.1$ and (b) $t = 0.8$. For $t = 0.1$, close to the multi-critical point on the critical line exists a small region ($v_\theta < v < v_\theta + \epsilon$) of the first order phase transitions (where the globule in the bulk and the adsorbed chain coexist) which ends at the point depicted by the small dash. Beyond the dash ($v > v_\theta + \epsilon$) the transition at the critical line is continuous, and corresponds to the attached semi-compact chain.

4. Monte Carlo renormalization group calculation

In this section we are going to apply the Monte Carlo renormalization group (MCRG) method to calculate the critical exponents ν and ϕ for 3d SG fractals with $b \geq 5$. First, we shall present the MCRG calculation of the critical exponent ν . In order to find the SAW critical exponent ν , in the bulk phase, we should determine the nontrivial fixed points of the RG transformations (2.8) and (2.9), and then we should solve the corresponding eigenvalue problem of the linearized RG transformations, that is, we

should solve the equation

$$\left| \begin{pmatrix} \frac{\partial A'}{\partial A} - \lambda_\nu & \frac{\partial A'}{\partial B} \\ \frac{\partial B'}{\partial A} & \frac{\partial B'}{\partial B} - \lambda_\nu \end{pmatrix} \right|^* = 0, \quad (4.1)$$

where the asterisk means that all derivatives should be taken at the corresponding fixed point and the superscript prime is used instead of the superscript $(r+1)$. Knowing the relevant eigenvalue λ_ν , we can determine the critical exponent ν using the formula (3.4). To learn a specific value of ν , for a given b , one should first find the coefficients $a(N_A, N_B)$, and $b(N_A, N_B)$ in the RG equations (2.8) and (2.9). As it was detailed in the previous sections, it has been possible to calculate the exact values of these coefficients only for $b \leq 4$. Thus, to get an entire sequence of values of ν for $b \geq 5$, we are going to circumvent the problem of explicit determination of the exact coefficients in the RG equations by applying the MCRG technique.

The MCRG method, allows direct calculation of derivatives that appear in the eigenvalue equation (4.1). It starts by locating the bulk nontrivial fixed points, which requires, at the beginning, implementation of a MC simulation of the SAWs for a chosen initial set of values (A_0, B_0) . In other words, we let the walker start his walking, at one fixed corner of the fractal generator and record the other corner, at which it leaves the generator, together with recording the total numbers N_A and N_B , of crossings of the A , or B , type through the elementary tetrahedron. The SAW walker crosses an elementary tetrahedron in the A (or B) way (see Fig. 3) with the weight (probability) A_0 , and B_0 , respectively. We repeat this MC simulation L times, for the same set (A_0, B_0) . Thus we find how many times the walker has passed through the generator in the A (or B) way and by dividing the corresponding numbers by L we get the values of the functions (2.8) and (2.9), denoted here by $A'(A_0, B_0)$ and $B'(A_0, B_0)$.

In this way we get the value of the sums (2.8) and (2.9) without specifying the coefficients $a(N_A, N_B)$, and $b(N_A, N_B)$. Then, the subsequent values A_n and B_n ($n \geq 1$), at which the MC simulation should be performed, can be found by using the generalized “homing” procedure [10, 11, 12], which can be terminated at the stage when the differences $A_n - A_{n-1}$ and $B_n - B_{n-1}$ become less than the statistical uncertainties associated with A_{n-1} and B_{n-1} , respectively. Consequently, fixed point (A^*, B^*) can be identified with the last value (A_n, B_n) found in this procedure.

Having learnt the fixed point, we need to solve the eigenvalue equation (4.1) in order to find the critical exponent ν via the formula (3.4). Thus, we should find the partial derivatives $\partial Y' / \partial X$ (where $X, Y \in \{A, B\}$) at the fixed point. For instance, starting with (2.8) (in the notation in which the superscript prime is used instead of the superscript $(r+1)$) and by differentiating it with respect to A we get

$$\frac{\partial A'}{\partial A} = \sum_{N_A, N_B} N_A a(N_A, N_B) (A)^{N_A-1} (B)^{N_B}. \quad (4.2)$$

Treating now A' as the grand canonical partition function, for the ensemble of all possible SAWs that start at one fixed corner of the fractal generator and leave it at the other

one, we can write the corresponding ensemble average

$$\langle N_A(A, B) \rangle_{A'} = \frac{1}{A'} \sum_{N_A, N_B} N_A a(N_A, N_B) (A)^{N_A} (B)^{N_B}, \quad (4.3)$$

which can be directly measured in a MC simulation. Finally, comparing the last two equations, we can express one of the requisite derivatives in terms of the measurable quantity

$$\frac{\partial A'}{\partial A} = \frac{A'}{A} \langle N_A(A, B) \rangle_{A'}. \quad (4.4)$$

In a similar way one can find additional three derivatives, so that we can write the general formula

$$\frac{\partial Y'}{\partial X} = \frac{Y'}{X} \langle N_X \rangle_{Y'}, \quad (4.5)$$

where X and Y stand for any pair of quantities from the set $\{A, B\}$. In this way we can learn, through the MC simulations, the partial derivatives that appear in the eigenvalue equation (4.1). Consequently, calculating the above derivatives at the fixed point and solving the eigenvalue equation (4.1) we obtain

$$\lambda_\nu = \frac{\langle N_A \rangle_{A'}^* + \langle N_B \rangle_{B'}^*}{2} + \sqrt{\left(\frac{\langle N_A \rangle_{A'}^* - \langle N_B \rangle_{B'}^*}{2} \right)^2 + \langle N_A \rangle_{B'}^* \langle N_B \rangle_{A'}^*}, \quad (4.6)$$

which means that λ_ν has been expressed in terms of quantities that all are measurable through the Monte Carlo simulations. Accordingly, we can learn the value of the critical exponent ν through the formula (3.4). We have applied this technique for a sequence of the 3d SG fractals and in Table 2 we present our findings for $2 \leq b \leq 40$, for the extended chain (in the bulk phase) fixed point (A_E, B_E) together with the related critical exponent ν_E . As one can see from Table 2 the fixed point values for B_E , decrease much faster than the values for A_E , when b increases. This means that we may neglect parameter $B^{(r)}$ (compared with $A^{(r)}$) for larger b , that is for $b > 12$. In order to estimate the influence of the parameter $B^{(r)}$ on the values of the critical exponent ν , we calculated, by the MCRG method, critical exponent ν for $b = 12$ with $B_E = 0$. We obtained the following result $\nu = 0.5989 \pm 0.0003$, which deviate 0.03% from the value $\nu = 0.5987 \pm 0.0003$ (see Table 2) found using the nonzero value of $B^{(r)}$. Concerning the analogous results for the collapse transitions (θ critical point) in the bulk phase, we have to point out that the corresponding point (A_θ, B_θ) cannot be located because the initial part of the applied technique (the “homing procedure”) does not possess the needed convergence.

We now apply the MCRG method to find the crossover critical exponent ϕ (which determines the number of adsorbed monomers) for the polymer phase, on the 3d SG fractals, described by the symmetric fixed point (3.8). To this end, we have to solve the eigenvalue problem for the second part (that starts with the third equation) of the RG

transformations (2.8)–(2.12), which reduces to solving of the equation

$$\begin{vmatrix} \left(\frac{\partial A'_1}{\partial A_1} - \lambda_\phi \right) & \frac{\partial A'_1}{\partial A_2} & \frac{\partial A'_1}{\partial B_1} \\ \frac{\partial A'_2}{\partial A_1} & \left(\frac{\partial A'_2}{\partial A_2} - \lambda_\phi \right) & \frac{\partial A'_2}{\partial B_1} \\ \frac{\partial B'_1}{\partial A_1} & \frac{\partial B'_1}{\partial A_2} & \left(\frac{\partial B'_1}{\partial B_1} - \lambda_\phi \right) \end{vmatrix}^* = 0. \quad (4.7)$$

Here the asterisk indicates that all derivatives should be taken at the symmetric fixed point $(A_E, B_E, A_E, A_E, B_E)$. The above equation gives, in general, three eigenvalues for each b , but in practice it turns out that only one of them (to be henceforth denoted by λ_ϕ) is relevant. Knowing λ_ϕ we can determine the critical exponent ϕ through the formula

$$\phi = \frac{\ln \lambda_\phi}{\ln \lambda_\nu}. \quad (4.8)$$

Hence, in an exact RG evaluation of ϕ one needs to calculate partial derivatives of sums (2.10)–(2.12), and thereby one should find the coefficients $a_1(N_A, N_B, N_{A_1}, N_{A_2}, N_{B_1})$, $a_2(N_A, N_B, N_{A_1}, N_{A_2}, N_{B_1})$, and $b_1(N_A, N_B, N_{A_1}, N_{A_2}, N_{B_1})$ by an exact enumeration of all possible SAWs for each particular b , which has been accomplished for fractals with $b \leq 4$. However, for $b \geq 5$, as in the case of the bulk phase, the exact enumeration turns out to be a formidable task. We have circumvent this problem by applying the MCRG method. Within this method, the first step would be to locate the symmetric fixed point. Fortunately, because of the structure of the symmetric fixed, the results given in Table 2 provide the complete information for this fixed point for a sequence of fractals with $2 \leq b \leq 40$. The next step in the MCRG method consists of finding λ_ϕ , without explicit calculation of the RG equation coefficients.

To solve the eigenvalue problem (4.7), so as to learn λ_ϕ , we need to find the requisite partial derivatives. These derivatives can be related to various averages of the numbers N_{A_1} , N_{A_2} , and N_{B_1} , of different SAW parts (of the types A_1 , A_2 and B_1) within a SAW path. Indeed, we may apply the relation (4.5) where here X and Y stands for any pair of quantities from the set $\{A_1, A_2, B_1\}$. Therefore, to calculate the derivatives (4.5) for $X, Y \in \{A_1, A_2, B_1\}$ at the symmetric fixed point, one needs the nine averages $(\langle N_{A_1} \rangle_{A'_1}^*, \langle N_{A_2} \rangle_{A'_1}^*, \langle N_{B_1} \rangle_{A'_1}^*, \langle N_{A_1} \rangle_{A'_2}^*, \langle N_{A_2} \rangle_{A'_2}^*, \langle N_{B_1} \rangle_{A'_2}^*, \langle N_{A_1} \rangle_{B'_1}^*, \langle N_{A_2} \rangle_{B'_1}^*, \langle N_{B_1} \rangle_{B'_1}^*)$, which are all measurable through MC simulations. Solving numerically the eigenvalue equation (4.7) we obtain λ_ϕ , and, finally, using relation (4.8), we find the values of the critical exponent ϕ (in the extended polymer phase), which are presented in Table 2, and discussed in the following paragraph.

First, we would like to compare the results obtained, via the exact RG approach and through the MCRG technique, for the first three members ($b = 2, 3, 4$) of the SG fractal families (given in Table 1 and Table 2, respectively). One can observe that the MCRG results for the critical exponents ν and ϕ deviate at most 0.2% from the exact results. This very good agreement provides confidence in applying the MCRG

Table 2. The MCRG ($2 \leq b \leq 40$) results obtained in this work for the bulk fixed-point value parameters A_E and B_E , and the SAW critical exponents ν_E and ϕ_E for the 3d SG family of fractals. Each entry of the table has been obtained by performing 10^5 requisite Monte Carlo simulation.

b	(A_E, B_E)	ν_E	ϕ_E
2	(0.4311 \pm 0.0009, 0.0505 \pm 0.0023)	0.6742 \pm 0.0051	0.7484 \pm 0.0152
3	(0.3421 \pm 0.0004, 0.0245 \pm 0.0015)	0.6543 \pm 0.0021	0.7148 \pm 0.0037
4	(0.2898 \pm 0.0004, 0.0122 \pm 0.0020)	0.6414 \pm 0.0012	0.6901 \pm 0.0036
5	(0.2560 \pm 0.0004, 0.0067 \pm 0.0019)	0.6315 \pm 0.0010	0.6707 \pm 0.0028
6	(0.2319 \pm 0.0003, 0.0038 \pm 0.0012)	0.6239 \pm 0.0009	0.6496 \pm 0.0024
7	(0.2148 \pm 0.0003, 0.0020 \pm 0.0018)	0.6169 \pm 0.0006	0.6333 \pm 0.0019
8	(0.2016 \pm 0.0003, 0.0012 \pm 0.0026)	0.6130 \pm 0.0005	0.6198 \pm 0.0016
9	(0.1912 \pm 0.0004, 0.0007 \pm 0.0008)	0.6087 \pm 0.0006	0.6023 \pm 0.0017
10	(0.1829 \pm 0.0003, 0.0005 \pm 0.0023)	0.6048 \pm 0.0003	0.5894 \pm 0.0013
12	(0.1703 \pm 0.0004, 0.0001 \pm 0.0035)	0.5987 \pm 0.0003	0.5686 \pm 0.0012
15	(0.1581 \pm 0.0001, -)	0.5933 \pm 0.0002	0.5385 \pm 0.0010
17	(0.1526 \pm 0.0001, -)	0.5899 \pm 0.0002	0.5213 \pm 0.0010
20	(0.1462 \pm 0.0001, -)	0.5869 \pm 0.0002	0.5014 \pm 0.0012
25	(0.1399 \pm 0.0001, -)	0.5817 \pm 0.0002	0.4666 \pm 0.0008
30	(0.1353 \pm 0.0001, -)	0.5804 \pm 0.0002	0.4325 \pm 0.0008
35	(0.1327 \pm 0.0001, -)	0.5759 \pm 0.0001	0.4275 \pm 0.0007
40	(0.1305 \pm 0.0001, -)	0.5755 \pm 0.0001	0.3765 \pm 0.0007

approach for a longer sequence of fractals ($5 \leq b \leq 40$). For the sake of a better assessment of the global behavior of the critical exponents ν and ϕ , as a function of the fractal scaling parameter b , we depict the corresponding values (from Tables 1 and 2) in Fig. 5 and Fig. 6, respectively. One can see that ν , being a monotonically decreasing function of b , crosses the narrow range determined by the predictions made for the three-dimensional Euclidean lattices, starting with $\nu = 7/12 = 0.5833$ [13], passing through the values 0.5850 [14] and 0.5874 [15], and ending with $\nu = 0.5882$ [16]. Crossing the interval of the possible Euclidean values for the exponent ν occurs at the scaling fractal parameter $b = 20$. Interestingly, one may observe from Fig. 6 that the exponent ϕ , being monotonically decreasing function of b , crosses the estimated three-dimensional Euclidean value $\phi = 1/2$ [17] also at $b = 20$.

5. Conclusion

In this paper we studied the adsorption phenomenon of a linear polymer, in a good and bad solvent, on impenetrable boundaries of fractal containers modelled by the 3d SG family of fractals. Each member of the 3d SG fractal family has a fractal impenetrable 2d adsorbing boundary (which is, in fact, 2d SG fractal surface) and can be labelled by an integer b ($2 \leq b \leq \infty$). For the first three members ($b = 2, 3, 4$) of the 3d fractal family we have performed exact RG analysis. This analysis enabled us to establish the phase diagrams (for fractals with $b = 3$ and $b = 4$; the $b = 2$ case was studied previously

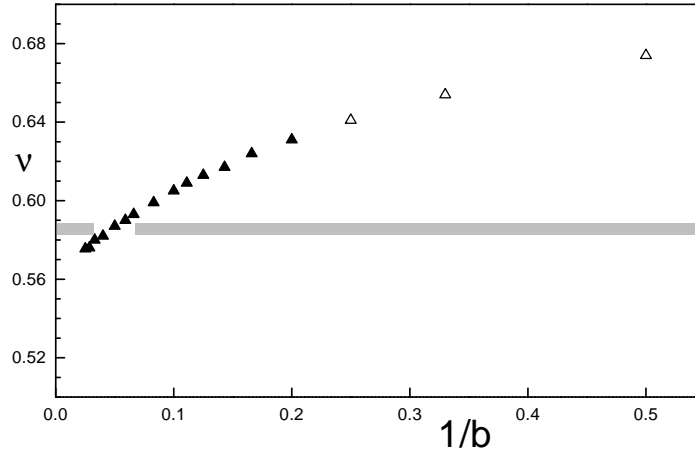


Figure 5. Data for the end-to-end critical exponent ν for the 3d SG family of fractals. The exact RG results are represented by open triangles, while the MCRG results are depicted by solid triangles. The shaded horizontal band represents the region of estimated values (found in the literature) for the three-dimensional Euclidean critical exponent ν . The error bars related to the MCRG data are not depicted in the figure since in all cases they lie within the corresponding symbols.

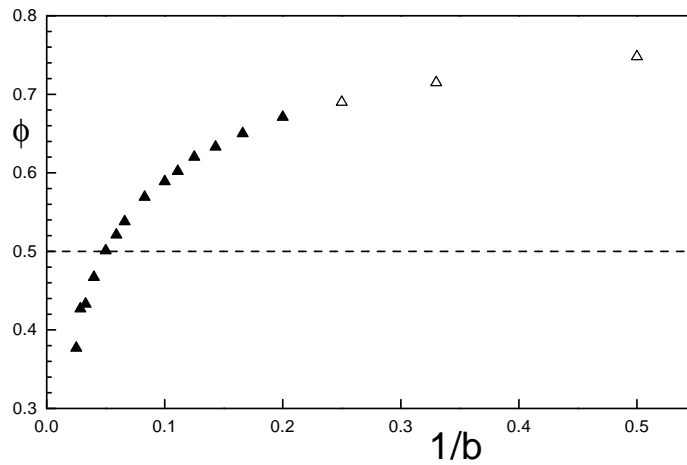


Figure 6. Data for the adsorption critical exponent ϕ for the 3d SG family of fractals. The exact RG results are represented by open triangles, while the MCRG results are depicted by solid triangles. The dashed horizontal line represents the putative universal Euclidean value $1/2$ of crossover critical exponent ϕ . The error bars related to the MCRG data are not depicted in the figure since in all cases they lie within the corresponding symbols.

[5]), which turned out to be very rich from the physical point of view. Indeed, the phase diagrams disclose six different polymer phases that merge together at a multicritical point, whose nature for $b = 3$ and $b = 4$, as well as the shape of the critical line that separates adsorbed from desorbed phases, depend on the value of the parameter t (associated with the monomer energy in the layer adjacent to the adsorbing boundary), which was not the case for $b = 2$. By analyzing the obtained phase diagrams we may conclude that similar diagrams can be expected for $b > 4$, but finding their exact pictures presently is not feasible.

By applying the exact and Monte Carlo renormalization group (MCRG) method, we calculated the critical exponents ν (associated with the mean squared end-to-end distance of polymers) and ϕ (associated with the number of adsorbed monomers) for a sequence of fractals with $2 \leq b \leq 4$ (exactly) and $2 \leq b \leq 40$ (Monte Carlo). The reliability of the MCRG results is manifested by the fact that in the cases $b = 2, 3, 4$ the MCRG results for ν and ϕ deviate at most 0.2% from the exact results. Unfortunately, it was possible to implement this powerful (MCRG) method only in the case of the extended polymer phase.

We find that, in the region studied, both ν and ϕ monotonically decrease with increasing b (that is, with increasing of the container fractal dimension d_f), and the very interesting fact that both functions, $\nu(b)$ and $\phi(b)$, cross the estimated Euclidean values at, approximately, the same value of the scaling parameter ($b \approx 20$). Here we would like to point out that in the case of the 2d SG fractals both exponents ν and ϕ also cross the corresponding Euclidean values, but not at the same value of b (at $b \approx 27$ for ν [11], while at $b \approx 6$ for ϕ [18]).

On the whole, our findings should be useful in making the corresponding 3d models of the polymer adsorption phenomena in porous media. Besides, our results may serve as beneficial in constructing theories of the polymer adsorption phenomena for the homogeneous 3d lattices, where so far, to the best of our knowledge, an exact approach has not been made.

Acknowledgments

This paper has been done as a part of the work within the project No.1634 funded by the Serbian Ministry of Science, Technology and Development.

Appendix A. RG equations for the surface parameters in the case of the three-dimensional $b = 3$ SG fractals

In this Appendix we give the exact RG equations for the surface RG parameters A_1 , A_2 and B_1 in the case of the 3d $b = 3$ SG fractal. We have found that these equations have the following form:

$$A'_1 = \sum_{i=0}^4 F_{A_1}^i(A_1, A_2, B, B_1) A^i, \quad (\text{A.1})$$

$$A'_2 = \sum_{i=0}^4 F_{A_2}^i(A_1, A_2, B, B_1) A^i, \quad (\text{A.2})$$

$$B'_1 = \sum_{i=0}^4 F_{B_1}^i(A_1, A_2, B, B_1) A^i, \quad (\text{A.3})$$

where

$$F_{A_1}^0(A_1, A_2, B, B_1) = A_1^3 + 3A_1^4 + A_1^5 + 2A_1^6,$$

$$F_{A_2}^0(A_1, A_2, B, B_1) = B^4 A_1 A_2^2 (44A_2 + 132A_1 A_2 + 132A_1 B_1 + 352A_1^2 B_1),$$

$$F_{B_1}^0(A_1, A_2, B, B_1) = B^4 (22A_2^3 + 132A_1^2 A_2^2 B_1 + 484A_1^3 A_2 B_1^2 + 484A_1^3 B_1^3),$$

$$F_{A_1}^1 = 2A_1 A_2^2 + 9A_1^2 A_2^2 + 10A_1^3 A_2^2 + 10A_1^4 A_2^2 + 8A_1^2 A_2 B_1 + 16A_1^3 A_2 B_1 + 20A_1^4 A_2 B_1 + 12A_1^2 B_1^2 + 6A_1^3 B_1^2 + 32A_1^4 B_1^2 + B^2(6A_2^4 + 14A_1 A_2^4 + 20A_1^2 A_2^4 + 64A_1 A_2^3 B_1 + 32A_1^2 A_2^3 B_1 + 40A_1 A_2^2 B_1^2 + 304A_1^2 A_2^2 B_1^2 + 320A_1^2 B_1^4),$$

$$F_{A_1}^2 = A_2^2 + 4A_1 A_2^2 + 9A_1^2 A_2^2 + 16A_1^3 A_2^2 + 14A_1^4 A_2^2 + 3A_2^4 + 9A_1 A_2^4 + 12A_1^2 A_2^4 + 8A_1^2 A_2 B_1 + 36A_1^3 A_2 B_1 + 40A_1^4 A_2 B_1 + 4A_2^3 B_1 + 24A_1 A_2^3 B_1 + 40A_1^2 A_2^3 B_1 + 12A_1^3 B_1^2 + 30A_1^4 B_1^2 + 24A_1 A_2^2 B_1^2 + 88A_1^2 A_2^2 B_1^2 + 48A_1 A_2 B_1^3 + 112A_1^2 A_2 B_1^3 + 128A_1^2 B_1^4 + B(4A_1 A_2^2 + 12A_1^2 A_2^2 + 8A_1^3 A_2^2 + 16A_1^4 A_2^2 + 4A_2^4 + 24A_1 A_2^4 + 40A_1^2 A_2^4 + 8A_1^2 A_2 B_1 + 32A_1^3 A_2 B_1 + 8A_1^4 A_2 B_1 + 12A_2^3 B_1 + 48A_1 A_2^3 B_1 + 120A_1^2 A_2^3 B_1 + 24A_1^2 B_1^2 + 64A_1^4 B_1^2 + 64A_1 A_2^2 B_1^2 + 176A_1^2 A_2^2 B_1^2 + 176A_1 A_2 B_1^3 + 352A_1^2 A_2 B_1^3 + 264A_1^2 B_1^4) + B^2(6A_2^2 + 12A_1^2 A_2^2 + 36A_1^3 A_2^2 + 20A_2^4 + 44A_1 A_2^4 + 24A_1^2 A_2 B_1 + 24A_1^3 A_2 B_1 + 96A_1^4 A_2 B_1 + 64A_1 A_2^3 B_1 + 232A_1^2 A_2^3 B_1 + 36A_1^3 B_1^2 + 36A_1^4 B_1^2 + 168A_1 A_2^2 B_1^2 + 168A_1^2 A_2^2 B_1^2 + 928A_1^2 A_2 B_1^3),$$

$$F_{A_1}^3 = 2A_2^2 + 8A_1 A_2^2 + 29A_1^2 A_2^2 + 42A_1^3 A_2^2 + 34A_1^4 A_2^2 + 4A_2^4 + 10A_1 A_2^4 + 14A_1^2 A_2^4 + 2A_2^6 + 28A_1^2 A_2 B_1 + 72A_1^3 A_2 B_1 + 96A_1^4 A_2 B_1 + 4A_2^3 B_1 + 24A_1 A_2^3 B_1 + 44A_1^2 A_2^3 B_1 + 4A_2^5 B_1 + 24A_1^2 B_1^2 + 30A_1^3 B_1^2 + 100A_1^4 B_1^2 + 26A_1 A_2^2 B_1^2 + 116A_1^2 A_2^2 B_1^2 + 16A_2^4 B_1^2 + 64A_1 A_2 B_1^3 + 112A_1^2 A_2 B_1^3 + 124A_1^2 B_1^4 + 136A_2^2 B_1^4 + B(4A_2^2 + 12A_1 A_2^2 + 28A_1^2 A_2^2 + 40A_1^3 A_2^2 + 40A_1^4 A_2^2 + 24A_2^4 + 48A_1 A_2^4 + 76A_1^2 A_2^4 + 20A_2^6 + 24A_1^2 A_2 B_1 + 112A_1^3 A_2 B_1 + 88A_1^4 A_2 B_1 + 32A_2^3 B_1 + 136A_1 A_2^3 B_1 + 192A_1^2 A_2^3 B_1 + 48A_2^5 B_1 + 24A_1^2 B_1^2 + 24A_1^3 B_1^2 + 136A_1^4 B_1^2 + 96A_1 A_2^2 B_1^2 + 768A_1^2 A_2^2 B_1^2 + 160A_2^4 B_1^2 + 448A_1 A_2 B_1^3 + 352A_1^2 A_2 B_1^3 + 944A_1^2 B_1^4 + 1320A_2^2 B_1^4),$$

$$\begin{aligned}
F_{A_1}^4 &= 2 A_2^2 + 8 A_1 A_2^2 + 26 A_1^2 A_2^2 + 36 A_1^3 A_2^2 + 32 A_1^4 A_2^2 + 8 A_2^4 + 26 A_1 A_2^4 + \\
&\quad 32 A_1^2 A_2^4 + 24 A_1^2 A_2 B_1 + 72 A_1^3 A_2 B_1 + 80 A_1^4 A_2 B_1 + \\
&\quad 8 A_2^3 B_1 + 64 A_1 A_2^3 B_1 + 116 A_1^2 A_2^3 B_1 + 24 A_1^2 B_1^2 + \\
&\quad 24 A_1^3 B_1^2 + 100 A_1^4 B_1^2 + 74 A_1 A_2^2 B_1^2 + \\
&\quad 236 A_1^2 A_2^2 B_1^2 + 112 A_1 A_2 B_1^3 + 336 A_1^2 A_2 B_1^3 + 292 A_1^2 B_1^4, \\
F_{A_2}^1 &= B(2 A_2^3 + 4 A_1 A_2^3 + 12 A_1^2 A_2^3 + 6 A_1^3 A_2^3 + 6 A_2^2 B_1 + 12 A_1 A_2^2 B_1 + \\
&\quad 32 A_1^3 A_2^2 B_1 + 24 A_1^2 A_2 B_1^2 + 44 A_1^3 B_1^3) + B^3(24 A_2^3 + \\
&\quad 88 A_1 A_2^3 + 88 A_1^2 A_2^3 + 168 A_1^3 A_2^3 + 32 A_2^5 + 84 A_1 A_2^5 + \\
&\quad 88 A_1 A_2^2 B_1 + 448 A_1^2 A_2^2 B_1 + 88 A_1^3 A_2^2 B_1 + 88 A_2^4 B_1 + \\
&\quad 132 A_1 A_2^4 B_1 + 640 A_1^3 A_2 B_1^2 + 920 A_1 A_2^3 B_1^2 + 320 A_2^2 B_1^3), \\
F_{A_2}^2 &= A_2 + 4 A_1 A_2 + 10 A_1^2 A_2 + 10 A_1^3 A_2 + 14 A_1^4 A_2 + 8 A_1^5 A_2 + 2 A_1^2 B_1 + \\
&\quad 8 A_1^3 B_1 + 4 A_1^4 B_1 + 18 A_1^5 B_1 + B(8 A_2^3 + 24 A_1 A_2^3 + \\
&\quad 36 A_1^2 A_2^3 + 32 A_1^3 A_2^3 + 12 A_2^5 + 12 A_1 A_2^5 + 36 A_1 A_2^2 B_1 + \\
&\quad 76 A_1^2 A_2^2 B_1 + 76 A_1^3 A_2^2 B_1 + 8 A_2^4 B_1 + 68 A_1 A_2^4 B_1 + 64 A_1^2 A_2 B_1^2 + \\
&\quad 88 A_1^3 A_2 B_1^2 + 48 A_2^3 B_1^2 + 88 A_1^3 B_1^3 + 304 A_1 A_2^2 B_1^3) + B^2(6 A_2 + \\
&\quad 12 A_1^2 A_2 + 36 A_1^3 A_2 + 12 A_1^4 A_2 + 24 A_1^5 A_2 + 36 A_2^3 + 56 A_1 A_2^3 + \\
&\quad 104 A_1^2 A_2^3 + 96 A_1^3 A_2^3 + 50 A_2^5 + 68 A_1 A_2^5 + 12 A_1^2 B_1 + \\
&\quad 24 A_1^4 B_1 + 12 A_1^5 B_1 + 12 A_2^2 B_1 + 88 A_1 A_2^2 B_1 + 160 A_1^2 A_2^2 B_1 + \\
&\quad 296 A_1^3 A_2^2 B_1 + 72 A_2^4 B_1 + 252 A_1 A_2^4 B_1 + 168 A_1 A_2 B_1^2 + \\
&\quad 216 A_1^2 A_2 B_1^2 + 168 A_1^3 A_2 B_1^2 + 160 A_2^3 B_1^2 + 328 A_1 A_2^3 B_1^2 + \\
&\quad 328 A_1^3 B_1^3 + 132 A_2^2 B_1^3 + 952 A_1 A_2^2 B_1^3) \\
F_{A_2}^3 &= 2 A_2 + 4 A_1 A_2 + 12 A_1^2 A_2 + 16 A_1^3 A_2 + 16 A_1^4 A_2 + 12 A_1^5 A_2 + 8 A_2^3 + \\
&\quad 24 A_1 A_2^3 + 42 A_1^2 A_2^3 + 26 A_1^3 A_2^3 + 4 A_1^2 B_1 + 8 A_1^3 B_1 + 8 A_1^4 B_1 + \\
&\quad 20 A_1^5 B_1 + 4 A_2^2 B_1 + 36 A_1 A_2^2 B_1 + 68 A_1^2 A_2^2 B_1 + 92 A_1^3 A_2^2 B_1 + \\
&\quad 20 A_1 A_2 B_1^2 + 76 A_1^2 A_2 B_1^2 + 112 A_1^3 A_2 B_1^2 + 120 A_1^3 B_1^3 + \\
&\quad B(4 A_2 + 8 A_1 A_2 + 24 A_1^2 A_2 + 32 A_1^3 A_2 + 32 A_1^4 A_2 + \\
&\quad 24 A_1^5 A_2 + 22 A_2^3 + 64 A_1 A_2^3 + 100 A_1^2 A_2^3 + 86 A_1^3 A_2^3 + 14 A_2^5 + \\
&\quad 32 A_1 A_2^5 + 8 A_1^2 B_1 + 16 A_1^3 B_1 + 16 A_1^4 B_1 + 40 A_1^5 B_1 + \\
&\quad 6 A_2^2 B_1 + 60 A_1 A_2^2 B_1 + 236 A_1^2 A_2^2 B_1 + 208 A_1^3 A_2^2 B_1 + 28 A_2^4 B_1 + \\
&\quad 28 A_1 A_2^4 B_1 + 64 A_1 A_2 B_1^2 + 88 A_1^2 A_2 B_1^2 + 304 A_1^3 A_2 B_1^2 + \\
&\quad 320 A_1 A_2^3 B_1^2 + 132 A_1^3 B_1^3 + 132 A_2^2 B_1^3), \\
F_{A_2}^4 &= 2 A_2 + 4 A_1 A_2 + 12 A_1^2 A_2 + 16 A_1^3 A_2 + 16 A_1^4 A_2 + 12 A_1^5 A_2 + 10 A_2^3 + \\
&\quad 30 A_1 A_2^3 + 50 A_1^2 A_2^3 + 40 A_1^3 A_2^3 + 8 A_2^5 + 12 A_1 A_2^5 + 4 A_1^2 B_1 + \\
&\quad 8 A_1^3 B_1 + 8 A_1^4 B_1 + 20 A_1^5 B_1 + 6 A_2^2 B_1 + 40 A_1 A_2^2 B_1 + \\
&\quad 94 A_1^2 A_2^2 B_1 + 112 A_1^3 A_2^2 B_1 + 20 A_2^4 B_1 + 58 A_1 A_2^4 B_1 +
\end{aligned}$$

$$\begin{aligned}
& 20 A_1 A_2 B_1^2 + 68 A_1^2 A_2 B_1^2 + 108 A_1^3 A_2 B_1^2 + 36 A_2^3 B_1^2 + \\
& 92 A_1 A_2^3 B_1^2 + 100 A_1^3 B_1^3 + 32 A_2^2 B_1^3 + 192 A_1 A_2^2 B_1^3, \\
F_{B_1}^1 = & B(3 A_1^2 A_2^3 + 8 A_1^3 A_2^3 + 6 A_1^3 A_2^2 B_1 + 44 A_1^3 A_2 B_1^2 + 66 A_1^2 B_1^3) + \\
& B^3(44 A_1 A_2^3 + 44 A_1^2 A_2^3 + 22 A_2^5 + 320 A_1^3 A_2^2 B_1 + 66 A_2^4 B_1 + \\
& 120 A_1 A_2^4 B_1 + 312 A_1^2 A_2 B_1^2 + 312 A_1^3 A_2 B_1^2 + 160 A_1 A_2^3 B_1^2 + \\
& 968 A_1^3 B_1^3 + 968 A_1 A_2^2 B_1^3 + 4308 A_1 B_1^5), \\
F_{B_1}^2 = & A_1^3 A_2 + 7 A_1^4 A_2 + 8 A_1^5 A_2 + 15 A_1^4 B_1 + 8 A_1^5 B_1 + B(6 A_1 A_2^3 + \\
& 12 A_1^2 A_2^3 + 12 A_1^3 A_2^3 + 10 A_1 A_2^5 + 16 A_1^2 A_2^2 B_1 + 60 A_1^3 A_2^2 B_1 + \\
& 24 A_1 A_2^4 B_1 + 44 A_1^2 A_2 B_1^2 + 176 A_1^3 A_2 B_1^2 + 88 A_1 A_2^3 B_1^2 + \\
& 132 A_1^3 B_1^3 + 576 A_1 A_2 B_1^4) + B^2(6 A_1^3 A_2 + A_1^4 A_2 + \\
& 54 A_1^2 A_2^3 + 48 A_1^3 A_2^3 + 6 A_2^5 + 28 A_1 A_2^5 + 18 A_1^4 B_1 + \\
& 48 A_1^5 B_1 + 128 A_1^2 A_2^2 B_1 + 136 A_1^3 A_2^2 B_1 + 18 A_2^4 B_1 + \\
& 124 A_1 A_2^4 B_1 + 432 A_1^3 A_2 B_1^2 + 318 A_1 A_2^3 B_1^2 + 132 A_1^2 B_1^3 + \\
& 632 A_1^3 B_1^3 + 312 A_1 A_2^2 B_1^3 + 1936 A_1 A_2 B_1^4 + 1452 A_1 B_1^5), \\
F_{B_1}^3 = & 2 A_1^3 A_2 + 10 A_1^4 A_2 + 8 A_1^5 A_2 + 2 A_1 A_2^3 + 14 A_1^2 A_2^3 + 22 A_1^3 A_2^3 + \\
& 18 A_1^4 B_1 + 16 A_1^5 B_1 + 26 A_1^2 A_2^2 B_1 + 74 A_1^3 A_2^2 B_1 + \\
& 12 A_1^2 A_2 B_1^2 + 164 A_1^3 A_2 B_1^2 + 44 A_1^2 B_1^3 + 120 A_1^3 B_1^3 + \\
& B(4 A_1^3 A_2 + 20 A_1^4 A_2 + 16 A_1^5 A_2 + 4 A_2^3 + 12 A_1 A_2^3 + \\
& 33 A_1^2 A_2^3 + 24 A_1^3 A_2^3 + 8 A_2^5 + 36 A_1^4 B_1 + 32 A_1^5 B_1 + \\
& 72 A_1^2 A_2^2 B_1 + 174 A_1^3 A_2^2 B_1 + 18 A_2^4 B_1 + 48 A_1 A_2^4 B_1 + \\
& 88 A_1^2 A_2 B_1^2 + 352 A_1^3 A_2 B_1^2 + 66 A_1 A_2^3 B_1^2 + 66 A_1^2 B_1^3 + \\
& 592 A_1^3 B_1^3 + 312 A_1 A_2^2 B_1^3 + 1452 A_1 B_1^5), \\
F_{B_1}^4 = & 2 A_1^3 A_2 + 10 A_1^4 A_2 + 8 A_1^5 A_2 + A_2^3 + 6 A_1 A_2^3 + 17 A_1^2 A_2^3 + \\
& 16 A_1^3 A_2^3 + 3 A_2^5 + 8 A_1 A_2^5 + 18 A_1^4 B_1 + 16 A_1^5 B_1 + \\
& 26 A_1^2 A_2^2 B_1 + 72 A_1^3 A_2^2 B_1 + 7 A_2^4 B_1 + 32 A_1 A_2^4 B_1 + \\
& 44 A_1^2 A_2 B_1^2 + 202 A_1^3 A_2 B_1^2 + 64 A_1 A_2^3 B_1^2 + \\
& 66 A_1^2 B_1^3 + 230 A_1^3 B_1^3 + 100 A_1 A_2^2 B_1^3 + \\
& 440 A_1 A_2 B_1^4 + 472 A_1 B_1^5.
\end{aligned}$$

Appendix B. RG equations for the bulk parameters in the case of the three-dimensional $b = 4$ SG fractals

The exact recursion relations for the bulk RG parameters A and B in the case of the 3d $b = 4$ Sierpinski fractal have the following form

$$\begin{aligned}
A' = & A^4 + 12 A^5 + 62 A^6 + 220 A^7 + 782 A^8 + 2426 A^9 + 12 A^5 B + 128 A^6 B + \\
& 776 A^7 B + 3416 A^8 B + 13324 A^9 B + 18 A^4 B^2 + 72 A^5 B^2 + 432 A^6 B^2 +
\end{aligned}$$

$$\begin{aligned}
& 2736 A^7 B^2 + 13294 A^8 B^2 + 56004 A^9 B^2 + 19 A^5 B^3 + 1456 A^6 B^3 + \\
& 8704 A^7 B^3 + 48256 A^8 B^3 + 213968 A^9 B^3 + 36 A^4 B^4 + 688 A^5 B^4 + \\
& 6880 A^6 B^4 + 33264 A^7 B^4 + 173936 A^8 B^4 + 816 A^5 B^5 + 781456 A^7 B^7 + \\
& 4350864 A^8 B^7 + 2904 A^4 B^8 + 31616 A^5 B^8 + 248608 A^6 B^8 + \\
& 2047360 A^7 B^8 + 9995376 A^8 B^8 + 70400 A^5 B^9 + 779584 A^6 B^9 + \\
& 5688896 A^7 B^9 + 13632 A^6 B^5 + 10369 A^7 B^5 + 562192 A^8 B^5 + \\
& 640 A^4 B^6 + 1792 A^5 B^6 + 32432 A^6 B^6 + 250672 A^7 B^6 + 1552992 A^8 B^6 + \\
& 7712 A^5 B^7 + 98528 A^6 B^7 + 24273344 A^8 B^9 + 65568 A^4 B^{10} + \\
& 354336 A^5 B^{10} + 2960032 A^6 B^{10} + 11284384 A^7 B^{10} + 44440800 A^8 B^{10} + \\
& 139392 A^5 B^{11} + 6933440 A^6 B^{11} + 25364736 A^7 B^{11} + 20945408 A^8 B^{11} + \\
& 259424 A^4 B^{12} + 3408768 A^5 B^{12} + 7491712 A^6 B^{12}, \\
B' = & A^8 + 24 A^9 + 268 A^{10} + 1624 A^{11} + 6544 A^{12} + 20288 A^{13} + 50676 A^{14} + \\
& 103904 A^{15} + 173050 A^{16} + 225108 A^{17} + 215392 A^{18} + 134968 A^{19} + \\
& 42514 A^{20} + 328 A^9 B + 2584 A^{10} B + 13940 A^{11} B + 56768 A^{12} B + \\
& 188356 A^{13} B + 491496 A^{14} B + 1000000 A^{15} B + 1539632 A^{16} B + \\
& 1701920 A^{17} B + 1192152 A^{18} B + 397392 A^{19} B + 36 A^8 B^2 + \\
& 832 A^9 B^2 + 14176 A^{10} B^2 + 85720 A^{11} B^2 + 368404 A^{12} B^2 + \\
& 1199040 A^{13} B^2 + 2954904 A^{14} B^2 + 5370136 A^{15} B^2 + 6814424 A^{16} B^2 + \\
& 5299288 A^{17} B^2 + 1901008 A^{18} B^2 + 2112 A^8 B^3 + 17424 A^9 B^3 + \\
& 89344 A^{10} B^3 + 482272 A^{11} B^3 + 1965376 A^{12} B^3 + 5900928 A^{13} B^3 + \\
& 12721232 A^{14} B^3 + 18817920 A^{15} B^3 + 16698368 A^{16} B^3 + \\
& 6662824 A^{17} B^3 + 616 A^6 B^4 + 1584 A^7 B^4 + 6388 A^8 B^4 + \\
& 76968 A^9 B^4 + 523696 A^{10} B^4 + 2577592 A^{11} B^4 + 9113852 A^{12} B^4 + \\
& 23214816 A^{13} B^4 + 40127080 A^{14} B^4 + 41398192 A^{15} B^4 + \\
& 18548660 A^{16} B^4 + 12912 A^7 B^5 + 62560 A^8 B^5 + 451600 A^9 B^5 + \\
& 2759488 A^{10} B^5 + 11688304 A^{11} B^5 + 34977824 A^{12} B^5 + \\
& 70124768 A^{13} B^5 + 82557440 A^{14} B^5 + 41200784 A^{15} B^5 + \\
& 1584 A^6 B^6 + 45056 A^7 B^6 + 296744 A^8 B^6 + 2361856 A^9 B^6 + \\
& 12623808 A^{10} B^6 + 43429664 A^{11} B^6 + 102376032 A^{12} B^6 + \\
& 139837056 A^{13} B^6 + 78454776 A^{14} B^6 + 7744 A^6 B^7 + 133440 A^7 B^7 + \\
& 1858832 A^8 B^7 + 10467744 A^9 B^7 + 46337232 A^{10} B^7 + \\
& 126642624 A^{11} B^7 + 201751952 A^{12} B^7 + 126633376 A^{13} B^7 + \\
& 17232 A^5 B^8 + 54192 A^6 B^8 + 950784 A^7 B^8 + 8336624 A^8 B^8 + \\
& 42390624 A^9 B^8 + 139673656 A^{10} B^8 + 253941232 A^{11} B^8 + \\
& 172479256 A^{12} B^8 + 431776 A^6 B^9 + 6405824 A^7 B^9 + 32770448 A^8 B^9 +
\end{aligned}$$

$$\begin{aligned}
& 127799456 A^9 B^9 + 273263456 A^{10} B^9 + 204194352 A^{11} B^9 + \\
& 471328 A^5 B^{10} + 4395872 A^6 B^{10} + 21993584 A^7 B^{10} + \\
& 107371568 A^8 B^{10} + 262855104 A^9 B^{10} + 199987864 A^{10} B^{10} + \\
& 1224960 A^5 B^{11} + 17655616 A^6 B^{11} + 76932128 A^7 B^{11} + \\
& 220464528 A^8 B^{11} + 151443088 A^9 B^{11} + 3702272 A^4 B^{12} + \\
& 11642752 A^5 B^{12} + 66511552 A^6 B^{12} + 148524304 A^7 B^{12} + \\
& 99652120 A^8 B^{12} + 3748096 A^3 B^{13} + 30934336 A^5 B^{13} + \\
& 110065872 A^6 B^{13} + 26465392 A^7 B^{13} + 6830208 A^3 B^{14} + \\
& 30509600 A^4 B^{14} + 49942336 A^5 B^{14} + 20614528 A^3 B^{15} + 5153632 B^{16}.
\end{aligned}$$

References

- [1] For review see Jones R A L and Richards R W 1999 *Polymers at Surfaces and Interfaces* (New York: Cambridge University Press); Kawaguchi M and Takahashi A 1992 *Adv. Colloid Interface Sci.* **37** 219
- [2] Eisenriegler E 1993 *Polymers near Surfaces* (Singapore: World Scientific)
- [3] Rajesh R, Dhar D, Giri D, Kumar S and Singh Y 2002 *Phys. Rev. E* in print
- [4] Vrbová T and Whittington S G 1998 *J. Phys. A: Math. Gen.* **31** 3989
- [5] Bouchaud E and Vannimenus J 1989 *J. Physique* **50** 2931
- [6] Knežević M and Vannimenus J 1987 *J. Phys. A: Math. Gen.* **20** L969
- [7] Dhar D and Vannimenus J 1987 *J. Phys. A: Math. Gen.* **20** 199
- [8] Maričić J and Elezović–Hadžić S *Preprint* cond-mat/0205509
- [9] Elezović S, Knežević M and Milošević S *J. Phys. A: Math. Gen.* 1987 **20** 1215
- [10] Redner S and Reynolds P J 1981 *J. Phys. A: Math. Gen.* **14** 2679
- [11] Milošević S and Živić I 1991 *J. Phys. A: Math. Gen.* **24** L833
- [12] Milošević S and Živić I 1993 *J. Phys. A: Math. Gen.* **26** 7263
- [13] Hueter I *Preprint* math.PR/0108199
- [14] Grassberger P 1993 *J. Phys. A: Math. Gen.* **26** 2769
- [15] Prellberg T 2001 *J. Phys. A: Math. Gen.* **34** L599
- [16] Nidras P 1996 *J. Phys. A: Math. Gen.* **29** 7929
- [17] Grassberger P 1994 *J. Phys. A: Math. Gen.* **27** 4069
- [18] Živić I, Milošević S and Stanley H E 1994 *Phys. Rev. E* **49** 636